Emergence of high spin polarization of conductance in atomic-size Co-Au contacts

Ilia N. Sivkov,[1] Oleg O. Brovko,[1] Dmitry I. Bazhanov,[2] and Valeri S. Stepanyuk[1]
[1]*Max Planck Institute of Microstructure Physics, Halle, Germany*
[2]*Faculty of Physics, Lomonosov Moscow State University, Moscow 119899, Russia*
(Received 3 July 2013; revised manuscript received 12 February 2014; published 27 February 2014)

We present a first-principles study of spin-dependent electron transport through gold nanochains suspended between cobalt electrodes aimed at elucidating the electronic origin of the high magnetoresistance recently observed experimentally in such nanojunctions. Our nonequilibrium Green's function based calculations confirm the occurrence of high spin polarization of conductance in Co/Au/Co nanocontacts, which in some cases reaches 90%. Our analysis allows to relate such behavior to the hybridization of electronic orbitals of neighboring cobalt and gold atoms of the nanocontact. The results obtained give clear evidence of the presence of spin injection from Co electrodes into paramagnetic gold contacts.

DOI: 10.1103/PhysRevB.89.075436 PACS number(s): 73.63.Rt, 71.15.Mb, 75.75.−c

I. INTRODUCTION

In the last decades, great attention was paid to spintronics and investigation of spin-dependent currents in nanostructures, where quantum effects cannot be neglected due to the small size of the system. In such systems, transport characteristics and electronic properties are strongly dependent on the structure of the material at the atomic scale and the interaction between individual atoms [1–6].

Spintronics takes its roots in the discovery of the giant magnetoresistance (GMR) effect by Fert (1988) [7] and Grünberg (1989) [8]. Within a decade from the discovery, it became the basis for a multitude of electronic memory devices. With the progress in experimental techniques of nanoscience made, it recently became possible to investigate subnanoscale structures experimentally [9–11]. This opened a new physical perspective onto giant and tunneling magnetoresistances, since in these experiments, the conductance showed quantized behavior with a conductance quantum of $G_0 = 2e^2/h$. Such behavior usually indicates the formation of a single-atomic contact or an atomic wire. Quantity G_0 is a conductance of a single "electron channel" (e.g., one band) without scattering, that can be formed, e.g., by a single-atomic wire. Here, e is the electronic charge and h is the Planck constant. Spin-dependent transport phenomena in atomic-scale systems have been the target of active investigations in recent years [12–23]. Among other things, particular attention has been given to the effect of magnetic anisotropy and geometry on the point contact conductance [20,21] and the occurrence of high magnetoresistance therein [12,15,19].

In a recent work, Bernand-Mantel and coworkers [18] have found that transport through a paramagnetic gold cluster sandwiched between cobalt electrodes exhibits nonzero magnetoresistance, which is ascribed to the presence of spin injection from magnetic cobalt electrodes into the paramagnetic gold cluster and the consequent spin transfer to the other electrode. Since gold has a mean spin diffusion length of about 100 nm [24], it is not surprising that two ferromagnetic Co electrodes and an Au nanoparticle should exhibit magnetoresistive behavior, especially in the tunneling geometry, which is the case in the latter experiment. However, an experiment by Egle and coworkers [19] has shown that the magnetoresistance ratio values of a Co-Au-Co break junction are excessively high (up to 100% in contact regime and 14 000% in tunneling geometry). This suggests that the spin injection from one cobalt electrode into the gold cluster and its coherent transfer to the detecting electrode are extremely efficient in that particular system.

A very similar system (Cu, Al, or Si chains between Co electrodes) has been investigated theoretically in the past by Bagrets and coworkers [22]. In that study, however, no system was found to exhibit a magnetoresistance ratio exceeding 50% [25] which might be partially due to unrealistic unrelaxed geometries used (limitations of the employed method) thus underlining the uniqueness of the Co-Au combination to which our study is devoted.

In the present work, we study the above-mentioned system (a gold chain connecting cobalt electrodes) with fully *ab initio* means. It is shown that this system can indeed exhibit high spin polarization of conductance and high magnetoresistance, giving clear evidence of hybridization-driven spin injection into the gold contact from cobalt electrodes. We give theoretical explanation of such behavior and relate it to the strong interaction between cobalt and gold s-d states in the junction region. We furthermore trace the evolution of conductance as the contact is stretched.

II. METHOD

From the *ab initio* point of view, the conductance can be calculated in the spirit of the Landauer-Büttiker formalism [26]. According to it, conductance of a nanocontact in the case of zero-bias can be expressed through a sum of transmission probabilities T_i of individual transport channels at the Fermi level: $G = G_0 \sum_i T_i(E_f)$. When spin-polarized systems are considered, conductance, in absence of spin-flip scattering, is treated separately in two spin-states, each of which can have a conductance of up to $G_0/2$. If the contribution of one spin is less, than that of the other, one can speak of spin-polarized conductance. While the presence of spin-mixing phenomena in such relativistic system as gold nanocontacts cannot be discarded out-of-hand, recent works by Hardrat *et al.* [27] and Smogunov *et al.* [5,6] have shown that inclusion of spin-orbital (SO) effects only qualitatively affects the conductance. For example, it was shown that fully relativistic treatment of conductance through a Pt nanowire yields a 15%–20%

smaller spin polarizations of conductance as compared to scalar-relativistic calculations [6]. Thus here we constrain ourselves to scalar-relativistic treatment of the system without limiting the generality of attained conclusions.

All transport calculations in the present paper were performed with the SMEAGOL code [28,29], which uses Keldysh nonequilibrium Greens's function (NEGF) method combined with density functional theory (DFT) formalism, implemented in SIESTA code [30,31]. SMEAGOL and SIESTA use linear combination of atomic orbitals (LCAO) as wave function bases and Troullier-Martins pseudopotentials to describe the atomic cores [32]. As an exchange-correlation functional we used Perdew-Zunger's scheme of local density approximation LDA [33], which is known to well describe the structural and electronic properties of 5*d* systems. For temperature smearing, the Methfessel-Paxton method with 600 K was chosen. As the LCAO basis set we chose a double-ζ basis including *s* and *d* shells for both Co and Au with additional polarized orbital for *s* shells. Scalar-relativistic pseudopotentials with $3d$, $4s$ and $5d$, $6s$ valence orbitals were chosen for cobalt and gold, respectively. For transport calculations, upon checking the convergence, a 5×5 *k*-point grid in the plane perpendicular to the transport direction (*z* axis) was chosen. Relaxation of electrodes was performed with SIESTA code with $4 \times 4 \times 1$ and $4 \times 4 \times 3$ *k*-point meshes for electrode and contact relaxations, respectively.

The geometry used in calculations is shown in Fig. 1(a). The nanocontact was modeled by a three-atom gold chain suspended between hcp Co(001) tips. The tips were represented by Co pyramids containing ten atoms in two hcp layers. The pyramids themselves were adsorbed on hcp Co(001) slabs [34,35]. To accommodate electronic relaxations at the surface and mitigate the effect of the supercell interaction the slabs were taken to be eight-layers thick and 4×4 atoms in cross-section perpendicular to the transport direction, which is sufficient to decouple the supercell images of nanocontacts from each other. With respect to the axis of the nanocontact (passing through the gold atoms) the system had a C_{3v}

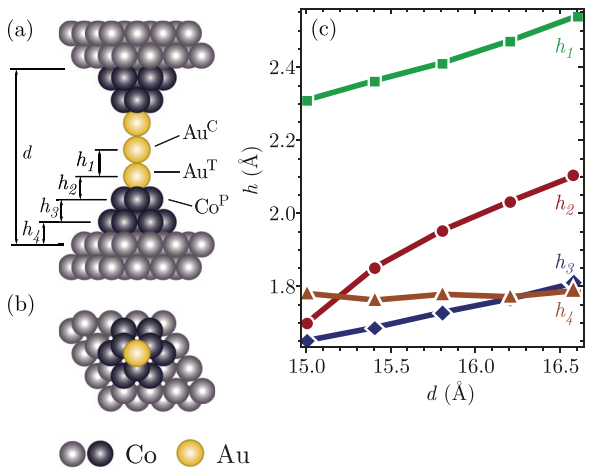

FIG. 1. (Color online) (a) Geometry of the nanocontact used in calculations: an Au wire between Co electrodes, side view. (b) Unit cell geometry of the electrode, top view. (c) Dependence of relaxed interlayer/interatomic distances h_i on the contact on the distance between electrodes *d*.

symmetry. In the following, we shall denote outer (tip) and central atoms of the gold chain as Au^T and Au^C respectively. The underlying pyramid cobalt atoms shall be denoted as Co^P. The distance between electrodes defying the stretching of the chain shall be referred to as *d*. In the following, we shall denote the systems by the distance between electrodes. In all calculations, the geometries of the electrodes and the gold chain were relaxed until the residual forces were no larger than 0.01 eV/Å.

III. RESULTS

To investigate the dependence of transport characteristics on the stretching of the contacts, calculations were performed at different distances *d* between the electrodes [see Fig. 1(a)], ranging from 15.00 to 16.6 Å. The geometry of the chain was kept linear during stretching. The dependence of relaxed interatomic distances in the contact on the distance between electrodes has a quite linear character [Fig. 1(c)]. The "softer" bonds between Au atoms, as well as the Au^T–Co^P bond closely follow the changes of *d*. The interlayer bonds in the pyramid are already much stiffer and the lower layer of the pyramid is almost unaffected by contact length change. This shows that the nature of interatomic bonds is not altered in the process of stretching and the orbital overlap can be expected to change likewise, i.e., smoothly. The restriction of the linearity of the chain is assumed solely for the sake of a clearer qualitative picture of the nanocontact physics. It shall be shown that fully unconstrained relaxation of the contact (allowing the chain to buckle and assume a zigzag configuration) does not significantly change the results and conclusions obtained.

Magnetic moments in the system are only weakly depend on the contact stretching. Bottom layer of the Co pyramids has a spin moment of $2.0\mu_B$ (for reference, hcp Co bulk value is $1.71\mu_B$), which shows no dependence on *d*. The moments of Co^P atoms increase from $2.11\mu_B$ to $2.19\mu_B$ as the contact is stretched from 15.0 to 16.6Å, reflecting the bond stretching and reduction of coordination. At the same time, the induced moment of Au^T atoms reduces from $0.11\mu_B$ to $0.05\mu_B$. Central gold atom Au^C is practically unpolarized at all stretching distances *d*.

A. Conductance

To set a starting point of our study of electronic and transport properties of the Co/Au/Co nanocontact, we consider the case when the magnetic moments of both Co leads are co-aligned. Within each electrode the spins of individual Co atoms are, of course, ferromagnetically coupled, hcp Co being a prototypical ferromagnet [34,35].

Calculated energy-resolved zero-bias transmission of the system described above [Fig. 1(a)] is shown in Fig. 2(a) for different interelectrode distances *d*. It can be seen that stretching of the contact has a pronounced influence on the energy position of the minority transmission peak, while majority conductance remains flat and almost unchanged. If we calculate the conductance polarization at the Fermi level as

$$P = \frac{T(E_f)^{\uparrow} - T(E_f)^{\downarrow}}{T(E_f)^{\uparrow} + T(E_f)^{\downarrow}},$$

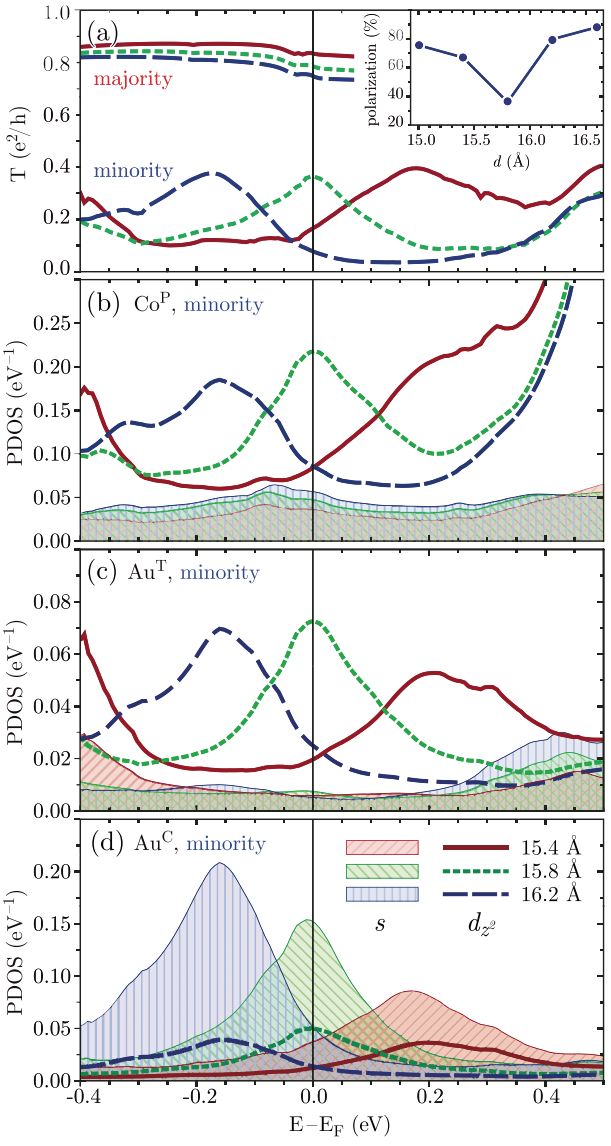

FIG. 2. (Color online) (a) Conductance of the nanocontact for different inter-electrode distances. The inset shows the spin polarization of conductance at the Fermi level. (b)–(d) Minority s and d projected densities of states for Co, tip Au, and central Au atoms for different distances between electrodes. Filled areas: s states, thick curves: d_{z^2} states. s-states curves for different distances are color- and hatching-coded (see the legend for details).

where $T^{\uparrow}$ and $T^{\downarrow}$ are the Fermi level transmission coefficients of majority and minority spin channels, respectively, we shall find [inset of Fig. 2(a)] that it is rather high, reaching 80% and furthermore changes significantly as the contact is stretched. High spin polarization of conductance is caused by the low amplitude of minority spin channel transmission around the Fermi level [see Fig. 2(a)] and therefore is a consequence of strong scattering of minority electrons. This result is quite interesting, since the density of states (DOS) of Co is dominated by the half-filled minority d band at the Fermi level and one could expect minority electrons to strongly contribute to Fermi-level transmission, as it is observed in pure Co nanojunctions [27,36].

Another effect that should be noted, is the strong change of the spin polarization of conductance with the stretching of the contact [inset in Fig. 2(a)]. It falls from almost 80% to 30% as the interelectrode distance is increased from 15.4 to 15.8 Å and is subsequently restored to almost 90% as the stretching continues towards 16.2 Å. From the energy resolved transmission curves [Fig. 2(a)] it can be deduced that this jump in polarization is caused by a pronounced peak in the transmission crossing the Fermi level in the minority channel as the contact is stretched. At the same time, majority transmission is comparable with G_0 and only slightly changes during stretching. Such closeness of the transmission coefficient to G_0 can be ascribed to the presence of ballistic transport in the majority channel.

To understand this behavior of transport properties, let us consider the projected density of states (PDOS) of the contact's gold (Au^C and Au^T) and neighboring cobalt atoms of the electrode Co^P [Figs. 2(b)–2(d)]. The majority states of the contact atoms, similarly to the majority transmission, are flat and featureless around the Fermi energy [shown in Fig. 3(a)]. They are mostly of s character and are not affected by the stretching of the contact. Their extended wave functions can provide transport almost without scattering due to the strong overlap (and robust band formation). Thus, to explain the conductance polarization, we shall concentrate on minority PDOS.

Comparing transmission and PDOS in Fig. 2, one immediately notices that the minority transmission peak can be correlated with the peaks in d_{z^2} states of Co^P and Au^T atoms as well as with s states of the Au^C atom. Other symmetries also show traces of hybridization, but to a significantly smaller degree and thus we do not show them here, so as not to overload the figures. Note that the amplitude of the d_{z^2}-states peak at the Co^P atom is several times larger than that of the same state at Au^T and Au^C atoms. The amplitude of the peak in s states of the Au^C atom, on the contrary, has the same order as the d_{z^2} states peak of Co^P. Appearance of the peaks in all contact atoms can be related to a hybridization of the Au^C atom's s states and the d_{z^2} states of Au^T and Co^P atoms. Large difference in amplitudes of the peaks in PDOS on Co^P and Au^T atoms is due to the fact that, firstly, gold atoms have practically no d states at the Fermi energy. Hybridization of Au^C and Au^T atoms is weak and therefore we observe the small amplitude of d_{z^2} peaks in Au^T atoms. And, secondly, Au^C atom's s states have long "tails" and can hybridize with cobalt d minority states directly.

To understand the origin of the peaks that we observe in Fig. 2, we shall take a look at the PDOS on a larger energy scale [Fig. 3(c)]. Analyzing the stretching-induced dynamics of the position of the peaks around −1.5 eV, and at the Fermi level, we see that the former shift to higher energies as the interelectrode distance is increased, while the latter shift downward. This behavior is consistent with the picture, where both sets of peaks belong to the same state split by the interatomic interaction (horizontal arrows). Thus, as the contact is stretched, the interatomic distance increases, reducing the orbital overlap and the states gradually coalesce into single atomic-like levels. So, the origin of these peaks that we observe in Fig. 2 can be the splitting of the sd_{z^2} hybridized

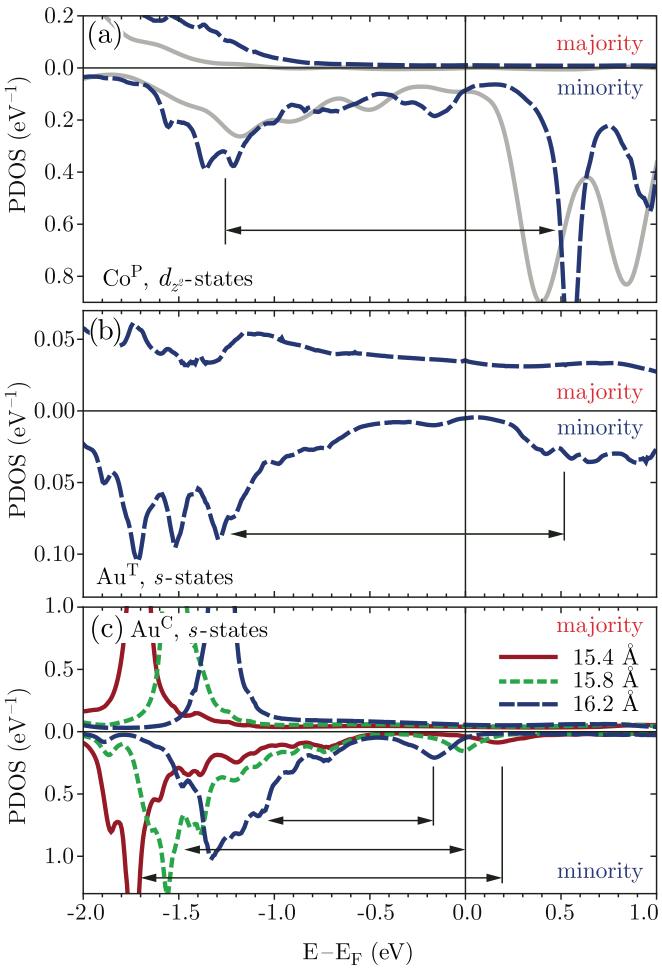

FIG. 3. (Color online) (a) Projected density of d_{z^2} states of Co atoms in contact with the Au wire (dashed line) and d_{z^2} states of the same atoms in absence of the Au chain (solid line). (b) s states of tip Au atom and (c) s states of central Au atom for different distances between electrodes. Positions of peaks around the fermi level are highlighted by vertical black lines. The splitting of the band/levels is shown by horizontal arrows.

state of the Au^C atom due to the interaction of the latter with its neighbors.

Though the physics described above gives a feasible explanation to the movement of the peak, it has to be mentioned, that there can be another possible explanation to the origin and movement of the peak close to the Fermi level. The s states of the gold chain can experience confinement between the two cobalt electrodes. As was shown in recent works [37–39], standing waves could exist in a chain nanocontact between electrodes and have a quantized spectrum. Therefore conductance may exhibit peaks at energies, corresponding to the energies of these confined states. However, the motion of the lower peak in Fig. 3(c) to higher energies (around −1.5 eV) would still have to be explained by the decrease of interaction between the central and the neighboring atoms.

A careful look at Figs. 3(a) and 3(b) will reveal that the minority states of the Au^T atom are dominated by the interaction with Co^P d_{z^2} states (dashed line). Comparing this density of states [Fig. 3(a), dashed line] with d_{z^2} states of the same electrode cobalt atom in absence of the chain [Fig. 3(a), solid line], we can see, that the structure of the DOS is similar. The only minor difference is in the position of the peaks above the Fermi level. For the single electrode these peaks are located closer to the Fermi level, than in the contact system. Primarily, the difference in positions of the peaks is explained by hybridization between cobalt and gold states. As the contact is stretched, the distances between the Au^T atom and underlying cobalt atoms change from 2.3 to 2.5 Å, which corresponds to the presence of a tight chemical s-d bond. Removing the gold tip atom obviously breaks that bond, leading to a shift of the d states of cobalt to lower energies.

In a recent theoretical work [20], it was shown that pure Co atomic-sized contacts show small spin polarization of the conductance at the Fermi level in contact regime. Nevertheless, in tunnel regime, the spin polarization reaches 100%. This effect comes from different decay lengths of majority (mostly of s character) and minority (d character) states of the contact. In the present case, d states of Co in minority channel also play the key role in conductance through the cobalt-gold contact. From Fig. 3(a), it can be also noted that d_{z^2} states of cobalt are partially filled and split into bonding and antibonding states. The hollow between them falls on the Fermi level, leaving it mostly depleted. The interaction between Au^T and Co^P atoms mostly manifests itself in the mixing of s and d_{z^2} states of these atoms. The s states of the Au^T atom are localized by the s-d hybridization, which "draws" them away from the Fermi energy, leaving the latter devoid of minority s electrons [Fig. 3(b)].

Putting together the puzzle, we can conclude that the Fermi level transmission of the contact is mostly determined by the s band in the majority channel. The d minority states are strongly localized and thus the conduction in the majority channel is dominant at the Fermi energy, resulting in a high positive polarization. Thus it can be said that s-d interaction at the Au-Co interface acts like as "blocking" mechanism for conductance in the minority channel. Similar effect has been reported in a theoretical study of Cu chains between planar Co leads [22]. Cu s states were shown to be the main channel of conductance at the Fermi level. However, due to the more localized nature of Cu s states as compared to gold, and likely due to the absence of a pyramid, in their study, the hybridization at the interface was much weaker, and consequently a much weaker magnetoresistance ratio was observed [15% versus 73% in our case (see Sec. III B)].

Taking one step back, we can summarize that the transport through a gold chain suspended between two Co electrodes is defined by the interaction between the Co and the tip Au atoms. High spin polarization of the conductance is caused by strongly suppressed minority and practically unaffected majority s states of the tip Au atom. Also significant contribution in conductance is made by peaks in d_{z^2} states of tip gold and neighboring Co atoms along with the s-states peak of the central atom. All of them appear due to interatomic orbital hybridization and form additional conductance channels in the contact. With the stretching of the contact, due to the weakening of the bonding between the atoms, the conductance peaks move in energy, altering the current polarization as they pass through the Fermi energy.

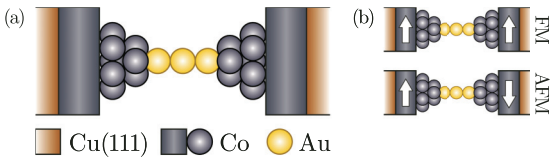

FIG. 4. (Color online) (a) Sketch of the nanojunction structure used for magnetoresistance calculations: Co/Au nanocontact attached to Cu(111) bulk leads. (b) Two spin alignments of electrodes used for magnetoresistance calculations.

B. Magnetoresistance

Having understood the electronic mechanisms determining the nanocontact's conductance, we now turn to a quantity, which is relevant for actual applications—the magnetoresistance. To estimate magnetoresistance ratio (MRR), we need to calculate conductance through the systems for the cases of parallel and antiparallel mutual alignments of the electrodes' magnetizations (see the right part of Fig. 4). Due to technical intricacies of the method, calculations for systems with differently aligned electrode magnetizations are rather unreliable (in the supercell part of the calculation a sharp domain wall occurs between one lead and the supercell image of the other one). Thus to estimate the MRR we replace semi-infinite Co electrodes with a Co slab deposited on a paramagnetic substrate (Fig. 4). As a nonmagnetic material for the substrate, we chose Cu, since the lattice of a Cu(111) surface is close to the hcp-stacked Co of our magnetic nanocontact. The same localized basis (with added p shells) was used for Cu as for Co and the whole system was allowed to relax with the same residual force restrictions as were applied for the Co electrodes (see Sec. II). The geometry of the contact pyramid and the Au chain were found to be not (or only negligibly) affected by the substitution of a part of Co with Cu.

To see whether the our Co/Au nanocontacts can be well approximated by the hybrid Cu/Co/Au system, we compare the conductance through both systems with parallel alignment of electrode magnetizations (Fig. 5). The energy-resolved conductance curves for both systems behave qualitatively the same. They have flat majority parts and strong depletions in the minority channels at the Fermi level. Thus, for all means and purposes, the hybrid Cu/Co/Au system seem to behave very

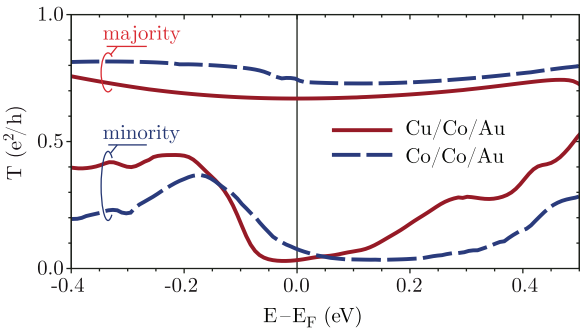

FIG. 5. (Color online) Comparison of the spin-polarized conductance of a system with semi-infinite Co electrodes (dashed blue line) and our model system for MR calculations—Co slabs supported on Cu (solid red line).

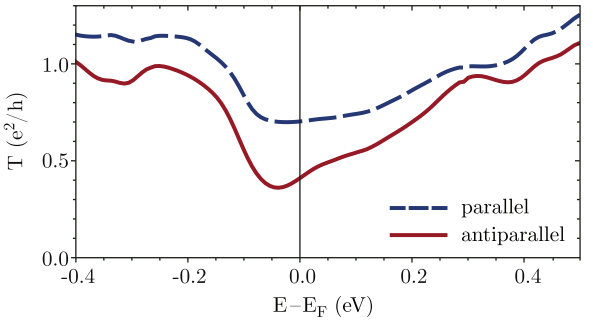

FIG. 6. (Color online) Total conductance for parallel and antiparallel spin orientations of cobalt electrodes.

similar to a system with bulk Co electrodes, which not only justifies the use of Cu/Co/Au systems for calculations but could also have important implications for the choice of the system geometry in the experiments. Additionally, the similarity in conductance between Co and Co/Cu leads further supports our statement about the defining role of the Co–Au interface in the formation of spin-polarized conductance.

Turning finally to the MRR, we calculate the energy resolved zero bias transmission for parallel and antiparallel lead-magnetization orientations for the nanocontact with $d = 15.4$ Å (dashed red and solid blue curves in Fig. 6, respectively). The Fermi-level transmission for the parallel configuration is found to be almost twice as high for the antiparallel one. In antiparallel configuration, Co-Au interaction between d and s states at the interface causes a decrease (or "blocking") of the conductance in both of channels. The MRR can be estimated from spin-resolved transmission coefficients as [15]

$$\mathrm{MRR} = \frac{T_{\uparrow\uparrow}(E_f) - T_{\uparrow\downarrow}(E_f)}{T_{\uparrow\downarrow}(E_f)},$$

where $T_{\uparrow\uparrow}(E_f)$ and $T_{\uparrow\downarrow}$ are the zero-bias transmissions at the Fermi level for parallel and antiparallel configurations of electrode magnetization alignments, respectively. In our case, we arrive at a value of 73%, which is close to the experimentally observed one.

C. Modified systems

It is also interesting to compare transport properties of systems with different chemical and geometrical structures. In Fig. 7, calculations of three such systems are presented. The first two systems have a linear geometry but different amounts of cobalt and gold in the contact [Figs. 7(a) and 7(b)]. The third system [Fig. 7(c)] has the same chemical structure as the system discussed in previous sections, but was allowed to assume a nonlinear configuration upon compression of the contact.

For the system with mixed cobalt-gold electrodes [Fig. 7(a)], where Co^P atoms were replaced with gold, the spin polarization was found to be less (about 50%) than in the original three-atom gold chain (90%). However, its sign remains the same as in the previous case. d states of cobalt atoms neighboring to gold in this system are similar to Co^P d states in the system with full cobalt electrodes, discussed

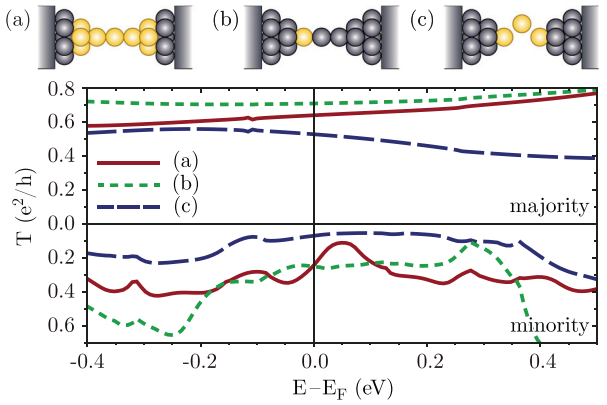

FIG. 7. (Color online) Conductance of systems with varying geometry and chemical composition/stoichiometry. Sketches of considered configurations are shown in the top part of the figure (atom colors the same as in Fig. 1). Corresponding conductance curves can be found in the graph in the bottom part.

in details above. Partially filled Co d_{z^2} states hybridize with s states of gold atoms, which leads to polarizations of these states. In contrast with the previously discussed case, here the gold atoms have a lower symmetry. So here not only d_{z^2}, but also d_{xz},d_{yz}-symmetry states of cobalt significantly contribute to the hybridization with gold and, consequently, to the conductance.

The system with mixed cobalt-gold wire between cobalt electrodes also shows high spin polarization (about 50%–70% depending on the stretching). It is found that the presence of cobalt atoms in a gold wire and on the tip of one of the electrodes does not affect the interaction of the pyramid cobalt atom with gold ones. We can see quite high spin polarization of conductance at the Fermi level [Fig. 7(b)], about 50%, which is a result of a depletion in s states at the tip gold atom, caused by s-d hybridization in minority channel between cobalt and gold.

Another example is a possible zigzag configuration of the gold chain [Fig. 7(c)]. In this case, the spin polarization of conductance at the Fermi level reaches 90% and the energy-dependent transmission coefficient behavior is practically identical to the one in the case of the linear gold contact. This is consistent with an idea that the s shell is spherically symmetric and not strongly susceptible to deviations from the linear geometry. In Ref. [22], a similar conclusion for Cu/Co nanocontacts has been reached. The intersite electron hopping in that case depends only on the distance between sites.

Finally, it is worth mentioning that Au is known as a material of choice to construct longer monatomic chains (up to 7–9 atoms). It is only logical to ask oneself, whether the effects discussed would still be valid for those longer nanojunctions. Indeed, our calculations have yielded the same high conductance polarization and MRR values for five-atom nanojunctions, which substantiates the generality of the physical mechanism described above.

IV. CONCLUSION

In a way of a more general summary, we can say that a metallic nanocontact with strong s-d hybridization can act as an extremely efficient spin filter with high magnetoresistance ratios, by far exceeding the values expected for nonmagnetic transitional metal systems. In the case of the nonmagnetic Au nanochain between Co electrodes, the interaction of s and d_{z^2} states at the cobalt-gold interface is responsible for a highly polarized conductance through the system, which can furthermore be tailored at will by stretching or compressing the junction. These results give a rigorous explanation of the efficient spin injection and high magnetoresistance ratios experimentally observed in Refs. [18] and [19].

ACKNOWLEDGMENTS

We would like to acknowledge the helpful discussions with Ivan Rungger. D.I.B. acknowledges RFBR for the financial support under Grant No. 13-02-01322.

[1] Y. V. Sharvin, J. Exp. Theor. Phys. **23**, 655 (1965).
[2] E. Scheer, P. Joyez, D. Esteve, C. Urbina, and M. H. Devoret, Phys. Rev. Lett. **78**, 3535 (1997).
[3] N. Agraït, A. L. Yeyatib, and J. M. van Ruitenbeek, Phys. Rep. **377**, 81 (2003).
[4] A. Smogunov, A. Dal Corso, A. Delin, R. Weht, and E. Tosatti, Nat. Nanotechnol. **3**, 22 (2008).
[5] A. Dal Corso, A. Smogunov, and E. Tosatti, Phys. Rev. B **74**, 045429 (2006).
[6] A. Smogunov, A. Dal Corso, and E. Tosatti, Phys. Rev. B **78**, 014423 (2008).
[7] M. N. Baibich, J. M. Broto, A. Fert, F. Nguyen Van Dau, F. Petroff, P. Eitenne, G. Creuzet, A. Friederich, and J. Chazelas, Phys. Rev. Lett. **61**, 2472 (1988).
[8] G. Binasch, P. Grünberg, F. Saurenbach, and W. Zinn, Phys. Rev. B **39**, 4828 (1989).
[9] H. Ohnishi, Y. Kondo, and K. Takayanagi, Nature (London) **395**, 2 (1998).
[10] A. I. Yanson, G. Rubio Bollinger, H. E. van den Brom, N. Agraït, and J. M. van Ruitenbeek, Nature (London) **395**, 783 (1998).
[11] J. I. Pascual, J. Méndez, J. Gómez-Herrero, A. M. Baró, N. Garcia, U. Landman, W. D. Luedtke, E. N. Bogachek, and H.-P. Cheng, Science **267**, 1793 (1995).
[12] D. Jacob, J. Fernández-Rossier, and J. J. Palacios, Phys. Rev. B **77**, 165412 (2008).
[13] M. R. Calvo, J. Fernández-Rossier, J. J. Palacios, D. Jacob, D. Natelson, and C. Untiedt, Nature (London) **458**, 1150 (2009).
[14] R. B. Pontes, E. Z. da Silva, A. Fazzio, and A. J. R. da Silva, J. Am. Chem. Soc. **130**, 9897 (2008).
[15] A. R. Rocha, T. Archer, and S. Sanvito, Phys. Rev. B **76**, 054435 (2007).

[16] K. Tao, I. Rungger, S. Sanvito, and V. S. Stepanyuk, Phys. Rev. B **82**, 085412 (2010).
[17] N. Néel, J. Kröger, and R. Berndt, Phys. Rev. Lett. **102**, 086805 (2009).
[18] A. Bernand-Mantel, P. Seneor, N. Lidgi, M. Muñoz, V. Cros, S. Fusil, K. Bouzehouane, C. Deranlot, A. Vaures, F. Petroff, and A. Fert, Appl. Phys. Lett. **89**, 062502 (2006).
[19] S. Egle, C. Bacca, H.-F. Pernau, M. Huefner, D. Hinzke, U. Nowak, and E. Scheer, Phys. Rev. B **81**, 134402 (2010).
[20] M. Häfner, J. K. Viljas, D. Frustaglia, F. Pauly, M. Dreher, P. Nielaba, and J. C. Cuevas, Phys. Rev. B **77**, 104409 (2008).
[21] M. Häfner, J. K. Viljas, and J. C. Cuevas, Phys. Rev. B **79**, 140410 (2009).
[22] A. Bagrets, N. Papanikolaou, and I. Mertig, Phys. Rev. B **70**, 064410 (2004).
[23] A. Bagrets, N. Papanikolaou, and I. Mertig, Phys. Rev. B **73**, 045428 (2006); **75**, 235448 (2007).
[24] Wen-C. Chiang, C. Ritz, K. Eid, R. Loloee, W. P. Pratt, Jr., and J. Bass, Phys. Rev. B **69**, 184405 (2004).
[25] Which might be partially due to unrealistic unrelaxed geometries used (limitations of the employed method).
[26] M. Büttiker, Y. Imry, R. Landauer, and S. Pinhas, Phys. Rev. B **31**, 6207 (1985).
[27] B. Hardrat, N.-P. Wang, F. Freimuth, Y. Mokrousov, and S. Heinze, Phys. Rev. B **85**, 245412 (2012).
[28] A. R. Rocha, V. M. García-Suárez, S. W. Bailey, C. J. Lambert, J. Ferrer, and S. Sanvito, Nat. Mater. **4**, 335 (2005).
[29] A. R. Rocha, V. M. García-Suárez, S. W. Bailey, C. J. Lambert, J. Ferrer, and S. Sanvito, Phys. Rev. B **73**, 085414 (2006).
[30] P. Ordejón, E. Artacho, and J. M. Soler, Phys. Rev. B **53**, R10441 (1996).
[31] J. M. Soler, E. Artacho, J. D. Gale, A. García, J. Junquera, P. Ordejón, and D. Sánchez-Portal, J. Phys.: Condens. Matter **14**, 2745 (2002).
[32] N. Troullier and J. L. Martins, Phys. Rev. B **43**, 1993 (1991).
[33] J. P. Perdew and A. Zunger, Phys. Rev. B **23**, 5048 (1981).
[34] B. W. Lee, R. Alsenz, A. Ignatiev, and M. A. Van Hove, Phys. Rev. B **17**, 1510 (1978).
[35] V. A. de la Peña O'Shea, I. D. P. R. Moreira, A. Roldán, and F. Illas, J. Chem. Phys. **133**, 024701 (2010).
[36] A. Smogunov, A. Dal Corso, and E. Tosatti, Phys. Rev. B **70**, 045417 (2004).
[37] E. G. Emberly and G. Kirczenow, Phys. Rev. B **60**, 6028 (1999).
[38] N. Nilius, T. M. Wallis, and W. Ho, Science **297**, 1853 (2002).
[39] V. S. Stepanyuk, P. Bruno, A. L. Klavsyuk, A. N. Baranov, W. Hergert, A. M. Saletsky, and I. Mertig, Phys. Rev. B **69**, 033302 (2004).